35th Annual International Conference of the IEEE EMBS
Osaka, Japan, 3 - 7 July, 2013

Free Induction Decay MR Signal Measurements toward Ultra-low Field MRI with an Optically Pumped Atomic Magnetometer*

Takenori Oida, *Member, IEEE* and Tetsuo Kobayashi, *Member, IEEE*

***Abstract*— Ultra-low field magnetic resonance imaging (ULF-MRI) has attracted attention because of its low running costs and minimum patient exposure. An optically pumped atomic magnetometer (OPAM) is a magnetic sensor with high sensitivity in the low frequency range, which does not require a cryogenic cooling system. In an effort to develop a ULF-MRI, we attempted to measure the free induction decay MR signals with an OPAM. We successfully detected the MR signals by combining an OPAM and a flux transformer, demonstrating the feasibility of the proposed system.**

I. Introduction

Optically pumped atomic magnetometers (OPAMs) are magnetic sensors with very high sensitivity in a spin exchange relaxation free condition, which is theoretically expected to be 0.01 fT/Hz$^{1/2}$ [1]. In addition, in magnetic field measurements, superconducting quantum interference devices (SQUIDs) have also very high sensitivity; however, SQUIDs require cryogenic cooling systems. In contrast, because OPAMs do not require a cryogenic cooling system, the running cost of OPAMs is expected to be lower. OPAMs are used in ultra-low field magnetic resonance imaging (ULF-MRI) and biomagnetic measurements for signal detection [2]–[4].

In general, high field has been used to improve the signal-to-noise ratio (SNR) and the spatial resolution in MRI. Recently, however, ULF-MRI has attracted attention because of its low running cost, smaller size, lighter weight, portability, and minimum patient exposure. In ULF-MRI, because of the low frequency of the MR signals, it is difficult to detect the MR signals with pickup coils, which are frequently used in high field MRI. In recent years, the studies on ULF-MRI with OPAMs or SQUIDs have progressed [2], [5], [6].

In this study, we fabricated a ULF-MR signal generation and detection system and carried out free induction decay (FID) MR signal measurements with an OPAM and a flux transformer (FT).

*Research supported the Innovative Techno-Hub for Integrated Medical Bio-imaging of the Project for Developing Innovation Systems, a Grant-in-Aid for Challenging Exploratory Research (22650221), and a Grant-in-Aid for Scientific Research A (24240081). All of them are from the Ministry of Education, Culture, Sports, Science and Technology (MEXT), Japan.

T. Oida is with Graduate School of Engineering, Kyoto University, Kyoto Daigaku Katsura, Nishikyo-ku, Kyoto 615-8510, Japan (corresponding auther to provide phone: +81-75-383-2259; fax: +81-75-383-2259; e-mail: oida@kuee.kyoto-u.ac.jp)

T. Kobayashi is with Graduate School of Engineering, Kyoto University, Kyoto Daigaku Katsura, Nishikyo-ku, Kyoto 615-8510, Japan (tetsuo@kuee.kyoto-u.ac.jp)

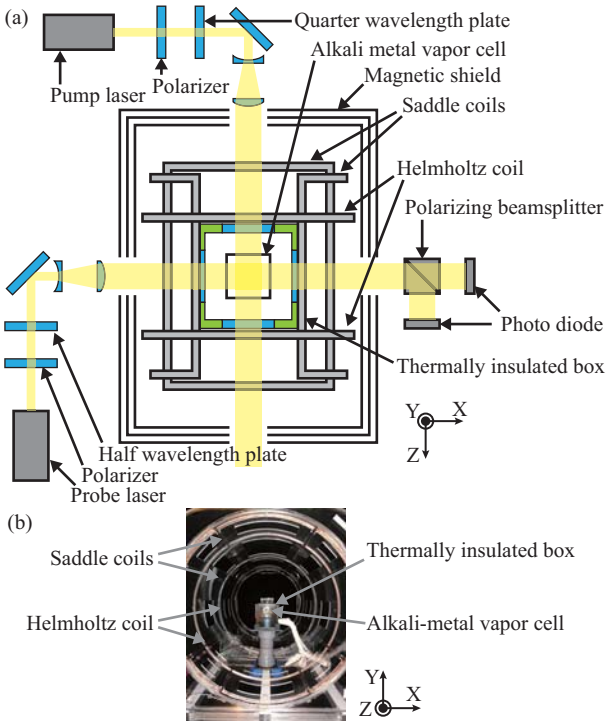

Figure 1. Schematic of an optically pumped atomic magnetometer (OPAM) (a) and an actual OPAM in a magnetic shield (b).

II. ULF-MRI with OPAMs

A. OPAM

An OPAM consists of a glass cell, which encapsulates alkali metal vapor and buffer gases, a pump laser, a probe laser, a heater, and a thermally insulated box, as shown in Fig. 1(a). The glass cell is placed in the center of two orthogonal saddle coils, and a Helmholtz coil to tune the bias magnetic field and to cancel the background magnetic field shown in Fig. 1(b).

In the OPAM, alkali metal vapor is formed by heating the glass cell. Then, the electron spin of alkali metal vapor is polarized by a circularly polarized pump laser beam, as shown in Fig. 2(a). When a bias magnetic field with the same direction as the pump laser beam (Z direction) and a magnetic field measured in the plane orthogonal to the pump laser beam (XY plane) are applied to high-density alkali metal vapor, the electron spins precess around the bias magnetic field, as shown in Fig. 2(b). The plane of the linearly polarized probe laser beam moves according to the magneto-optical effect, as shown in Fig. 2(c). Therefore,

978-1-4577-0216-7/13/$26.00 ©2013 IEEE

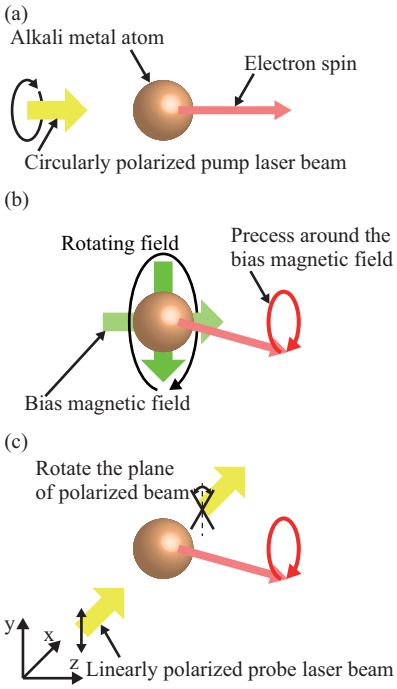

Figure 2. The principle of an OPAM.

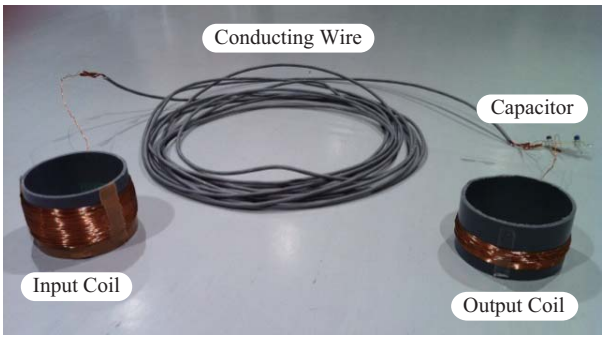

Figure 3. A flux transformer.

even a significantly weak magnetic field can be detected by measuring the plane of the linearly polarized probe laser beam.

B. ULF-MRI with OPAMs

MR signal detection in ULF-MRI is an application of magnetic field measurements with OPAMs [2]. In ULF-MRI, because of the low resonant frequency of the MR signals, it is difficult to detect the MR signals with the pickup coil that is used in clinical MRIs. In contrast, the OPAMs are highly sensitive to low frequencies. The frequency of a high-sensitive OPAM is changed by the amplitude of the bias magnetic field that is applied along the pump laser beam direction. When potassium vapor is used in an OPAM, the resonant angular frequency ω_K is expressed as follows,

$$\omega_K = \gamma_K B_K \tag{1}$$

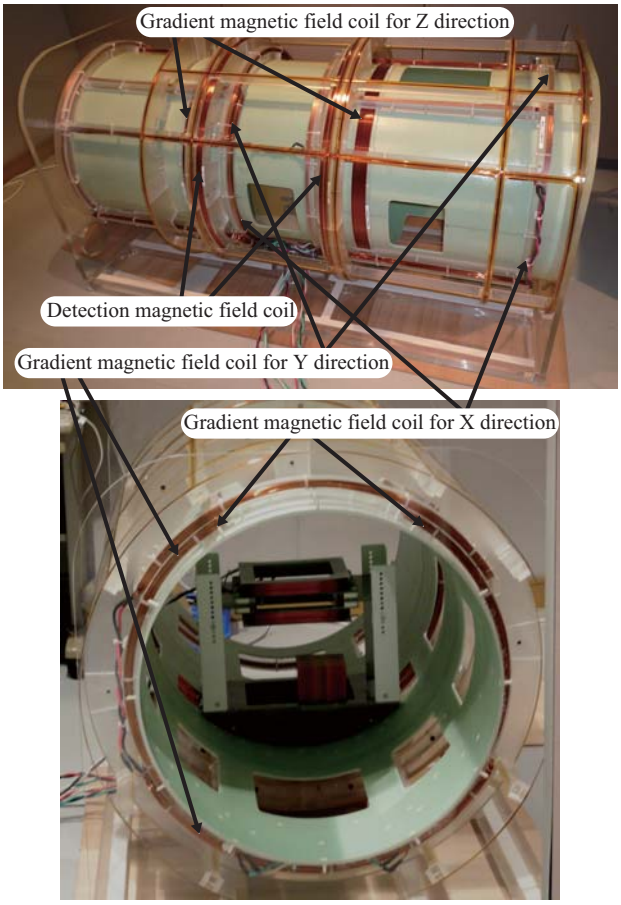

Figure 4. The magnetic field-applying coil system used in our ULF-MRI.

where γ_K and B_K are the gyromagnetic ratio of the electron spin for potassium and the bias magnetic field, respectively. The gyromagnetic ratio γ_K of the electron spin for potassium is approximately $2\pi \times 7.00 \times 10^9$ rad/T in the low frequency region. This gyromagnetic ratio is about 164 times greater than that of the nuclear spin for proton $\gamma_p = 2\pi \times 4.26 \times 10^7$ rad/T, which is most generally measured in clinical MRI. Therefore, the sensitivity of MR signal detection is limited when an object and an OPAM are placed in the same magnetic field.

Remote detection with an FT has been recently proposed as a solution to this problem [2]. An FT consists of an input coil, an output coil, and a tunable capacitor, as shown in Fig. 3. The resonant frequency of the FT can be tuned to that of the MR signals by the tunable capacitor. It has been reported that the SNR of MR signal detection of an OPAM and FT is improved by optimizing the radius and the number of turns and layers in the output coil of the FT and shortening the distance between the FT and OPAM [7]. However, the sensitivity of MR signal detection is limited by that of the FT, which is less sensitive than that of the OPAM [7].

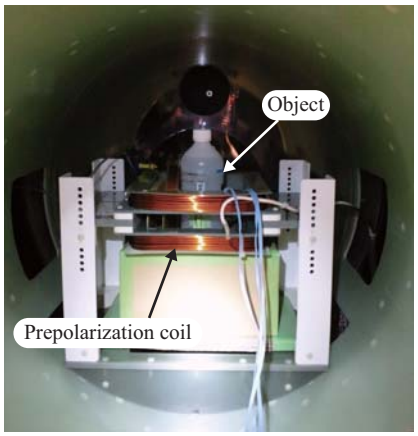

Figure 5. Prepolarization coil for strengthening the MR signal.

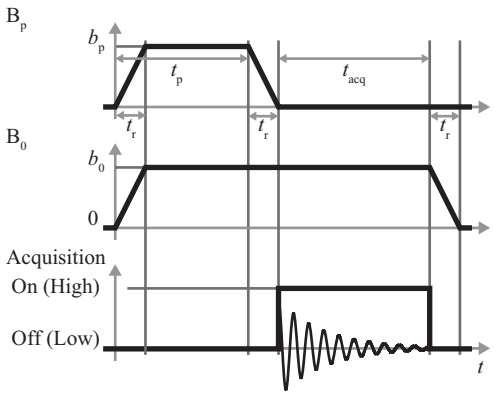

Figure 6. Pluse sequence for measuring free induction decay (FID) MR signal.

III. Experimental measurements of MR signals with an OPAM in ULF-MRI

A. MR signal generation system with a ULF

In this study, we fabricated a magnetic field applying system with a detection magnetic field coil and orthogonal gradient magnetic field coils in three directions, as shown in Fig. 4. In general, because the MR signals are proportional to the detection magnetic field, the MR signals generated by a ULF are significantly weaker than those generated by a high field. In this study, therefore, the prepolarizing magnetic field generated by the prepolarization coil shown in Fig. 5 was used to strengthen the magnetization generating MR signals. This coil was placed in the magnetic shielding case to reduce the background magnetic noise. In addition, to control this coil according to the pulse sequences generating the MR signals, the current supplied by the power amplifiers was controlled by a computer via a digital-to-analog (D/A) converter. MR signal generation or MRI is required to control the current of each coil with high accuracy; therefore, a D/A converter with an update cycle of up to 1 MHz was adopted. In this study, the FID MR signal $s(t)$, expressed by Eq. (2), was generated by the pulse sequence shown in Fig. 6 and the above mentioned ULF-MR signal generation system:

$$s(t) = A\exp(-\alpha t)\cos(\omega t - \theta) \tag{2}$$

where A, α, ω, and θ are the amplitude, damping factor, angular frequency, and initial phase of the signal, respectively. In this experiment, the detection magnetic field was tuned to generate the FID MR signal with a resonant frequency of 10 kHz (angular resonant frequency $\omega = 2\pi \times 10^4$). In addition, the other parameters of the pulse sequence shown in Fig. 6 were set, as listed in TABLE I.

B. MR signal detection system with an OPAM and FT

In this study, the FID MR signals generated by the MR signal generation system with the ULF mentioned in section III-A were detected by an MR signal detection system with an OPAM and FT. We used potassium vapor in the OPAM, a titanium-sapphire pump laser, and a distributed feedback laser as the probe laser. By placing the OPAM in the large magnetic shielding box, the achieved noise level of the magnetic signal detections with an OPAM was fT order at approximately 10 kHz. In addition, three orthogonal and homogeneous magnetic fields were applied to the glass cell of the OPAM for canceling the magnetic field along the X and Y direction, as shown in Fig. 1, and tuning the bias magnetic field along the pump laser beam direction (Z direction).

We used a single-layer solenoid coil, 72 mm inner diameter and 25 mm long, with 25 turns as the input coil of an FT. The output coil of the FT was a 10-layer solenoid coil with 130 turns and an inner diameter and length of 100 mm and 15 mm, respectively. The output coil of the FT was placed on the thermally insulated box. In this setting, the distance between the center of the glass cell and the output coil of the FT was 50 mm.

TABLE I
Parameter set used for measuring the FID MR signals

Pre-polarization field	**Amplitude (b_{p})**	approx. 32 mT
	Duration (t_{p})	15 s
Detection field	**Amplitude (b_0)**	approx. 234.87 μT
Acquisition	**Sampling frequency**	200 kHz
	Sampling time (t_{acq})	50 ms

C. Measurements of FID MR signals

In this study, the detection of the FID MR signal (a MR signal) was carried out with the MR signal generation and detection system mentioned in sections III-A and III-B. We used purified water in the experimental measurements. The frequency of the bias magnetic field of the OPAM was tuned at approximately 10 kHz, which corresponded to the resonant frequency of the FID MR signal. The end of the ramp down triggered the detection in the prepolarizing magnetic field, and the timing was expressed as 0 ms. The data were sampled from -25 ms to 25 ms with a sampling rate of 200 kHz.

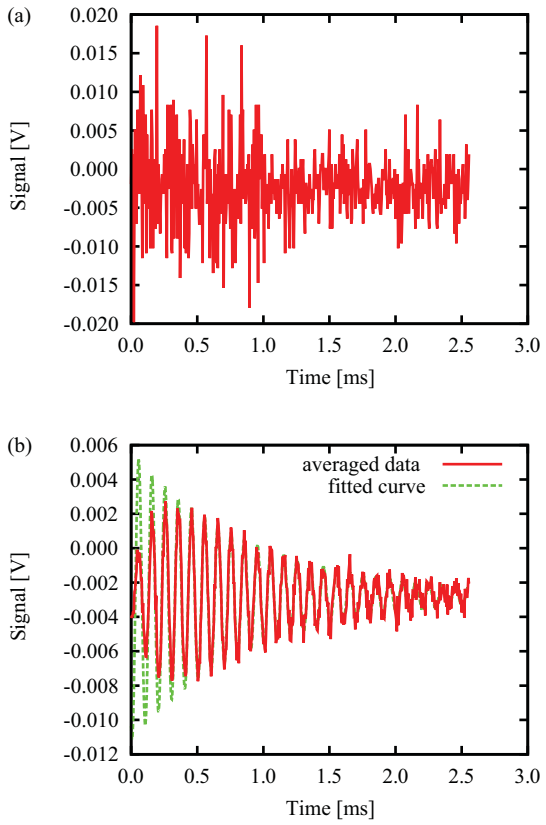

Figure 7. Results of measuring FID MR signals. An example of FID signals (a), and the averaged FID signal of 100 times.

This was repeated 100 times at an interval of 20 s and then averaged.

IV. Results and Discussion

The measured and the averaged ($n = 100$) FID MR signals are shown in Figs. 7(a) and 7(b), respectively. Both FID MR signals of 2.56 ms were extracted from the time when the ramp down of the prepolarizing magnetic field had ended, which included the data of 512 samples. In Fig. 7(b), the dashed line is the fitted curve of Eq. (2), which subtracted the DC component from the averaged FID MR signal.

Because the measured data have a large noise component, as seen in Fig. 7(a), a clear FID MR signal could not be confirmed. Although the magnetic noise was reduced by the magnetic shielding case, the magnetic noise generated by each coil of the MR signal generation system was attributed to the ripple currents and noise of the power amplifiers. In particular, the magnetic noise caused by the prepolarization coil, which was placed closest to the input coil of an FT, should be reduced to improve the SNR of the detection. In addition, since there may be more losses and noise in human bodies than those in the purified water phantom used in this study, the input coil of an FT should be optimized to reduce the losses and noise in the human bodies.

On the other hand, as seen from the averaged data in Fig. 7(b), FID MR signals could be generated by the system mentioned in III-A. This result confirmed that the MR signals could be detected with an OPAM and FT. From the fitting results, because the resonant frequency of the measured MR signal was 10.016 kHz, it was found that we could control MR signal generation with the error from the target frequency was less than 0.2%.

In the future work, optimization of the FT to improve the SNR of the detection, reduction of the magnetic noise caused by the coils of the MR signal generation system, and improvement in the sensitivity of an OPAM will be required toward ULF-MRI.

V. Conclusion

In this study of a ULF-MRI system, we carried out measurements of FID MR signals with an OPAM and FT. Because prepolarization and detection magnetic field could be accurately controlled, the MR signals were generated and detected with the pulse sequence in the proposed system. In the future, the sensitivity of the MR signal detection system with an OPAM and FT is expected to improve. In addition, the noise caused by the magnetic field applying system needs to be reduced.

Acknowledgment

We would like to express our heartfelt thanks to Dr. Ito for assistance and discussions.

References

[1] I. K. Kominis, T. W. Kornack, J. C. Allred, and M. V. Romalis, "A subfemtotesla multichannel atomicmagnetometer," *Nature*, vol. 422, pp. 596–599, 2003.

[2] I. M. Savukov, V. S. Zotev, M. A. Volegov, M. A. Espy, A. N. Matlashov, R. H. Gomea, and R. H. K. Jr., "Mri with an atomic magnetometer suitable for practical imaging applications," *Journal of Magnetic Resonance*, vol. 199, no. 2, pp. 188–191, 2008.

[3] S. Taue, Y.Sugihara, T. Kobayashi, S. Ichihara, K. Ishikawa, and N. Mizutani, "Development of a highly sensitive optically pumped atomic magnetometer for biomagnetic field measurements: A phantom study," *IEEE Transactions on Magnetics*, vol. 46, no. 9, pp. 3635–3638, 2010.

[4] K. Kamada, Y. Ito, and T. Kobayashi, "Human mcg measurements with high-sensitivity potassium atomic magnetometer," *Physiological Measurement*, vol. 33, pp. 1063–1071, 2012.

[5] F. Verpillat, M. P. Ledbetter, S. Xu, D. J. Michalak, C. Hilty, L.-S. Bouchard, S. Antonijevic, D. Budker, and A. Pines, "Remote detection of nuclear magnetic resonance with an anisotropic magnetoresistive sensor," *Proceedings of the National Academy of Sciences*, vol. 105, no. 7, pp. 2271–2273, 2007.

[6] J. Hatta, M. Miyamoto, Y. Adachi, J. Kawai, G. Uehara, and H. Kado, "Squid-based low field mri system for small animal," *IEEE Transactions on Applied Superconductivity*, vol. 21, no. 3, pp. 526–529, 2011.

[7] T. Oida, Y. Kawamura, and T. Kobayashi, "Optimization of flux transformer for ultra-low field mri systems with optically pumped atomic magnetometers," *IEEE Transactions on Magnetics*, vol. 47, no. 10, pp. 3074–3077, 2011.